Published in final edited form as:

Respir Physiol Neurobiol. 2017 February ; 236: 57–68. doi:10.1016/j.resp.2016.11.006.

Histological identification of phrenic afferent projections to the spinal cord

Jayakrishnan Nair[1,4], **Tatiana Bezdudnaya**[2], **Lyandysha Zholudeva**[2], **Megan R. Detloff**[2], **Paul J. Reier**[3,4], **Michael A. Lane**[2], and **David D. Fuller**[1,4]

[1]University of Florida, College of Public Health and Health Professions McKnight Brain Institute Department of Physical Therapy PO Box 100154, 100 S. Newell Dr, Gainesville, FL 32610

[2]Department of Neurobiology & Anatomy College of Medicine Drexel University 2900, W. Queen Lane, Philadelphia, PA 19129

[3]University of Florida, College of Medicine McKnight Brain Institute Department of Neuroscience PO Box 100244, 100 S. Newell Dr, Gainesville FL 32610

[4]Center for Respiratory Research and Rehabilitation, University of Florida, Gainesville, FL 32610

Abstract

Limited data are available regarding the spinal projections of afferent fibers in the phrenic nerve. We describe a method that robustly labels phrenic afferent spinal projections in adult rats. The proximal end of the cut phrenic nerve was secured in a microtube filled with a transganglionic tracer (cholera toxin β-subunit, CT-β, or Cascade Blue) and tissues harvested 96-hrs later. Robust CT-β labeling occurred in C3-C5 dorsal root ganglia cell bodies and phrenic afferent projections were identified in the mid-cervical dorsal horn (laminae I-III), intermediate gray matter (laminae IV, VII) and near the central canal (laminae X). Afferent fiber labeling was reduced or absent when CT-β was delivered to the intrapleural space or directly to the hemidiaphragm. Soaking the phrenic nerve with Cascade Blue also produced robust labeling of mid-cervical dorsal root ganglia cells bodies, and primary afferent fibers were observed in spinal grey matter and dorsal white matter. Our results show that the 'nerve soak' method effectively labels both phrenic motoneurons and phrenic afferent projections, and show that primary afferent project throughout the ipsilateral mid-cervical gray matter.

Keywords

spinal; phrenic; afferent; cholera toxin; cascade blue

1. Introduction

The phrenic nerve is comprised of approximately 50% somatic and sympathetic efferent fibers, and 50% sensory afferents (Landau *et al.*, 1962; Langford and Schmidt, 1983) (Goshgarian and Roubal, 1986a; Gottschall, 1981). Studies of axonal conduction velocity

Correspondence: David D. Fuller, Ph.D. ddf@phhp.ufl.edu Michael A. Lane, Ph.D. mlane.neuro@.gmail.com.

indicate that myelinated phrenic type Ia and II fibers innervate the crural region (Corda *et al.*, 1965b; Duron *et al.*, 1978; Glebovskii, 1962; Holt *et al.*, 1991; Marlot *et al.*, 1985), and Ib afferents innervate the costal region (Banzett *et al.*, 1981; Fryman and Frazier, 1987). Unmyelinated C-fibers are also prevalent in the phrenic nerve (Duron and Marlot, 1980; Jammes *et al.*, 1986; Langford and Schmidt, 1983). While the precise functional role of phrenic nerve afferents to the control of breathing and autonomic function remain a topic of ongoing investigation, multiple studies have confirmed powerful physiologic effects of phrenic afferent activation. For example, electrical or chemical stimulation of phrenic afferents can alter diaphragm blood flow (Hussain *et al.*, 1991), change phrenic (Formenti and Zocchi, 2014; Jammes *et al.*, 1986; Speck and Revelette, 1987) and intercostal motor output (De Troyer, 1998), and inhibit lumbosacral spinothalamic neurons (Bolser *et al.*, 1991). Polysynaptic projections from phrenic afferent neurons also project to the thalamus and are likely to contribute to the conscious perception of breathing (Davenport *et al.*, 1985; Zhang and Davenport, 2003). In contrast to the electrophysiological characterization of phrenic afferent function, little is known about the anatomical distribution of phrenic afferent projections within the spinal cord. To our knowledge, there are only a few published anatomical studies that have traced phrenic primary afferents to document their spinal distribution (Goshgarian and Roubal, 1986a; Larnicol *et al.*, 1984; Song *et al.*, 1999). The purpose of the present investigation was to histologically identify phrenic afferent projections in the cervical spinal cord of the adult rat. To accomplish this, we developed a method for soaking the phrenic nerve with a neuronal tracer, and compared the results with either direct application of the tracer to the diaphragm (Lane *et al.*, 2008) or delivery to the intrapleural space (Mantilla *et al.*, 2009) delivery. The results show more extensive spinal distribution of phrenic afferents than previously reported in adult animals (Goshgarian and Roubal, 1986b).

2. Materials and methods

2.1. Experimental animals

All animal care and experimental procedures were conducted with the University of Florida or Drexel University Institutional Animal Care and Use Committee (IACUC) approval and following NIH guidelines(National Research Council Committee on Guidelines for the Use of Animals in Neuroscience and Behavioral, 2003). A total of 35 adult Sprague-Dawley rats (20 males, 15 females) were obtained from Envigo Inc. (formally known as Harlan Scientific, Indianapolis, IN, USA) and housed in either the McKnight Brain Institute Animal Care Facility at the University of Florida, or the Queen Lane Campus of Drexel University (Philadelphia).

All survival surgical procedures used in this study were performed under general anesthesia (1.5-2% isoflurane in O_2). At the terminal time point, animals were deeply anesthetized and euthanized by intraperitoneal injection (0.4-0.5 ml) of pentobarbital sodium solution (390mg pentobarbital sodium and 50mg phenytoin sodium per ml). The animals were then transcardially perfuse-fixed with paraformaldehyde (4% w/v in 0.1 M phosphate buffer solution [PBS], pH 7.4) prior to tissue harvest.

2.2. Unilateral (left) phrenic nerve soak

A schematic illustrating the movement of the two transganglionic tracers used in this study to identify phrenic nerve afferent projection (*i.e.*, cholera toxin β-subunit (CT-β) and Cascade Blue) is provided in Fig. 1.

Unilateral (left) phrenic nerve soak with CT-β was performed in 8 rats. An approximately 2 cm long surgical incision was made on the ventral aspect of the left neck under deep isoflurane anesthesia. The layers of the neck muscles were separated using blunt dissection and a retractor was applied to expose the brachial plexus. The phrenic nerve was cut distally and a 3-4 mm Silastic tubule (1.47mm I.D. χ 1.96mm O.D.) was placed around the nerve. The proximal end of the tube was sealed with silicone elastomer, and a small amount of colored dye was added to visually inspect for leaks. The tube was then cleared and 4-5 μl of CT-β (1% solution, w/v in distilled water; MW~11.5 kDa, List Biological Laboratories, CA) was injected using a Hamilton syringe. The distal end of the tube was then sealed with silicone elastomer and the surgical field was closed and wound clips were applied. In an additional 3 rats, we performed C4 dorsal rhizotomy prior to the application of nerve soak. This was done to test the specificity of phrenic nerve soak in labeling afferents entering via DRG. For these experiments, we surgically removed C4 DRG and spared C3 and C5.

Analgesic medication (Buprenex) was given twice daily for 48 hours. No animals developed complications or showed signs of distress. Previous studies exploiting the transganglionic property of CT-β in peripheral nerve have used prolonged application of the neuronal tracer (*i.e.* 96 hours) for optimal afferent labeling (Shehab *et al.*, 2004; Wall *et al.*, 2002). Therefore, the animals were transcardially perfused 96 hours following CT-β labeling.

Studies using Cascade Blue® (Molecular Probes D7132, MW=3 kDa, 5% w/v in sterile physiological saline) were conducted by our collaborative team at Drexel University. Cascade Blue is a fluorescent molecule conjugated to a dextran molecule. The primary objective of these additional experiments was to confirm that the nerve soak method would be effective when used by an independent laboratory. An additional objective was to couple phrenic afferent labeling with additional immunochemistry, as follows. Antibodies against choline acetyltransferase (ChAT) were used to identify motoneuron soma and dendrites in the mid-cervical spinal cord in rats that had Cascade Blue applied to the phrenic nerve. This approach enabled definitive confirmation of dendritic labeling (dual-labeled for Cascade Blue and Chat) *vs.* phrenic afferent projections (labeled with Cascade Blue only. In addition, antibodies against calcitonin gene-related peptide (CGRP) and isolectin-B4 (IB4) were used to assess the distribution of small diameter (nociceptive) afferent projections relative to the expected distribution of large diameter (non-nociceptive) afferents in the cervical cord. The distribution of CGRP and IB4 labeled was afferent projections was compared with Cascade Blue positive afferents. Sections through the dorsal root ganglion (DRG) of these animals were also made to assess the distribution of Cascade Blue, CGRP and IB4 positive DRG neurons.

The Cascade Blue solution was applied via the phrenic nerve soak method as described above (n=10). Rats were then allowed to recover for 72 (n=3) or 96 hours (n=7) at which time they were terminally anesthetized and perfuse-fixed with paraformaldehyde (4% w/v in

0.1M PBS). Spinal cord and DRG tissues were dissected, cryoprotected (30% sucrose) and cut in cross-section (40 μm), and then histologically evaluated following immunochemistry to recognize Cascade Blue, IB4, CGRP, or ChAT (see 2.4. Immunochemistry).

In a subset of animals (n=2), the 1% CT-β solution was combined with Bartha strain of pseudorabies virus (PRV). PRV is a retrograde transsynaptic tracer that is highly effective in the phrenic motor system (Lane *et al.*, 2008). The recombinant used in this study was monomeric red fluorescent protein PRV614 ($2.0 \chi 10^8$ pfu/ml). A total of 5 μl PRV614 was added to the microtube with the 1% CT-β solution. The surgical procedure was the same as described earlier. The health of the PRV614 infected animals was monitored multiple times daily during the post-operative survival period. The animals co-labelled with PRV614 had the same 96-hr terminal end point as the other cohort. Thus, the intent was not to rigorously identify second order "pre-phrenic" interneurons as in prior work (Lane *et al.*, 2008), but rather to determine if the PRV method would work in conjunction with the CT-β approach.

2.3. Intrapleural and muscular application of CT-β

Unilateral intrapleural injection of CT-β and unilateral CT-β application to the hemi-diaphragm were each performed on 6 separate groups of rats. These experiments were done to determine if either an intrapleural or direct muscular application methods could also effectively label phrenic afferent projections in the spinal cord. Intrapleural injections were delivered under deep isoflurane anesthesia. The animals' rib cage was palpated and 15-20 μl of CT-β solution (1% w/v in distilled water) was injected on the left, fifth intercostal space (Mantilla *et al.*, 2009). Application of CT-β directly to the peritoneal surface of the diaphragm was done as described previously (Lane *et al.*, 2008). Briefly, under isoflurane anesthesia (2-3% in oxygen), an incision was made along the linea alba. The skin and the muscles covering the abdomen were retracted to expose the peritoneal surface of the diaphragm and 20 μl of the CT-β solution was topically applied to the left hemi-diaphragm using a sterile paint brush. The abdomen was closed by suturing the muscles (4-0 Vicryl) and wound clips applied to the skin.

2.4. Tracing controls

Rhizotomy of the mid-cervical (C4) dorsal roots was performed to selectively eliminate phrenic afferents projections arising from C4 while sparing both the C3 and C5 dorsal roots. The rhizotomy procedure was performed in sterile conditions under deep isoflurane anesthesia. The surgical approach was through the dorsal aspect of the neck. The muscles in the neck were carefully dissected and C3-C4 laminectomy was performed to expose the dorsal roots. The C4 dorsal roots were then sectioned using a microscissor. The wound was closed by suturing the muscle in layers, and the skin closed with wound clips. Analgesia (Buprenorphine, 0.03-0.05 mg/kg) was given twice per day for 2 days. After two days of recovery, phrenic afferents were labeled using the phrenic nerve soak procedure as described above.

2.5. Tissue preparation

Rats were transcardially perfused with 4% paraformaldehyde and both the spinal cord and mid-cervical DRGs were harvested within 1-2 days. The harvested spinal cords were post-

fixed in 4% paraformaldehyde in PBS overnight. Spinal cords and DRGs were then placed into 30% sucrose for dehydration and cryo-protection. Once the tissue sank to the bottom of the sucrose solution, the cords, and the DRG were removed and micro-dissected to remove the dura mater. The tissue was embedded separately in optimal cutting temperature compound (ThermoFisher Scientific, Pittsburgh, USA) using a cryomold. The cryomold was then placed in methylpentabutane cooled by dry ice. Once the tissue was frozen it was sectioned using a cryostat (10-40 μm).

2.6. Immunochemistry

Cross-sections of the spinal cord (slide mounted (20 μm) or free-floating (40 μm)) and longitudinal sections of DRGs (slide mounted (10 or 20 μm)) were treated for immunofluorescence (CT-β, Cascade Blue, CGRP and IB4). Sections were washed in PBS-Triton (0.1MPBS with 0.02% Triton-X, pH 7.4, 3×5 minutes), blocked against nonspecific protein labeling (10% serum in 0.1 mN PBS-Triton, 1-2 hours), and incubated at 4°C overnight with primary antibodies. Primary antibodies included: CT-β (1:2000, polyclonal goat anti-Cholera Toxin β subunit, List Laboratories, Product# 703), PRV (1:10,000; Rb133/Rb134 (antigen: whole, purified, acetone-inactivated PRV particles), provided by Dr. Lynn W. Enquist (Princeton University) as part of Virus Center funding (P40RR018604)), Cascade Blue (rabbit anti AlexaFluor-405/CascadeBlue, LifeTechnologies (A5760); 1:200), choline acetyl transferase (goat anti-ChAT, Millipore (AB144); 1:500), isolectin B4 (IB4; biotinylated lectin from griffonia simplicifolia, Sigma; 1:1000); calcitonin gene-related peptide (CGRP, guinea pig anti-alpha CGRP, Peninsula Laboratories International (T-5053); 1:1000). The following day, sections were washed in PBS-Triton (3×5 minutes) and then incubated with fluorescently conjugated secondary antibodies (1:500, Donkey α-Goat Rhodamine Red (AffiniPure Donkey α-Goat IgG, Jackson ImmunoResearch, PA, Lot#705-295-003) or Alexa 488 (donkey α-goat IgG, ThermoFisher Scientific, NY, Catalog# A-11055)). Immunohistochemical control experiments consisted of sections where either a non-specific Ig-Goat block antibody was used instead of primary antibody or the primary antibody was omitted entirely. These experiments confirmed that afferent fiber labeling only occurred when the tissues were incubated with the primary antibody (data not shown).

2.7. Microscopy

Sections were photographed and examined via an Olympus Cell Sens BX51 or Zeiss AxioImager M2 fluorescence microscope. The images were taken using a monochrome digital camera, pseudocolored within imaging software (Cell Sens BX51, Olympus or Zen Pro, Zeiss). In addition, a subset of tissue was processed for confocal microscopy using Olympus IX2-DSU Spinning Disk Confocal Fluorescent Microscope System (Tokyo, Japan). Individual images taken with the Olympus microscope were merged using Adobe Photoshop to create a composite image of the spinal cross section. Dual-labeled images taken with the Zeiss microscope were photographed in grey-scale, pseudo-colored, merged, and Z-stacks were flattened with an extended depth of field, using Zen 2012 software. Adobe Illustrator software (version 2015.2) was used to create camera lucida images of phrenic afferent projections.

3. Results

3.1. CT-β nerve-soak.

Robust phrenic motoneuron labeling was observed in the ventral C3–5 spinal cord. As shown in Fig. 2, phrenic motoneurons can be clearly identified as a distinct cluster with cytological and topographic features consistent with prior reports (Dobbins and Feldman, 1994; Goshgarian *et al.*, 1991; Lane *et al.*, 2008). Phrenic afferent projections could be clearly identified in mid-cervical spinal cord, and were distinguished by the punctate appearance of the labeling, the very thin diameter of the axonal projections and the presence of terminal boutons (Fig. 2B) (Wall *et al.*, 2002). The histological appearance of the afferent terminals was distinct from that of phrenic motoneuron dendrites as shown in Fig. 2C (see also results section 3.3 for confirmation of phrenic dendritic labeling *vs.* phrenic afferent projections).

Phrenic afferent fibers were observed in laminae I-III of the dorsal gray matter (Figs. 2 and 3), and extended into laminae IV-V and VI-VII (Fig. 3A-E). Phrenic afferent projections were observed in the central canal region (lamina X) in 2 of 8 rats (Fig. 3D). Additionally, in 1 spinal cord, a small cluster of CT-β positive afferent fibers was identified in the contralateral medial dorsal horn. No CT-β positive afferent projections were visualized in the region of phrenic motoneurons (lamina IX) in any animals (Fig. 3F). All rats in the nerve soak group showed positive CT-β labeling in C3-C5 DRG soma (Fig. 3G), thereby confirming that primary afferent neurons had taken up and transported the molecule. Camera lucida-style composite drawings are shown in Fig. 3H-J. These images show the typical pattern of CT-β-positive afferent projections to the C4 spinal cord in 3 different spinal cords. Note also that projections could be observed in the dorsal white matter, in the area of the fasciculus cuneatus. Additional histological images in which CT-β labeled cervical spinal tissues were stained with NeuN to recognize neuronal soma are provided in Fig. 4. These examples demonstrate phrenic motoneuron labeling (Fig. 4B), and afferent projections in lamina I-III (Fig. 4C-D) and IV-VII (Fig. 4E-F). The higher power images shown in Fig. 4G-H reveal terminals (synaptic boutons) of phrenic afferent projections in the vicinity of interneuron cell bodies.

Lastly, it should be noted that positive CT-β labeling was not observed in the mid-cervical dorsal horn of one animal despite an apparently successful initial surgical approach. However, on inspection of the microtube at the time of tissue harvest, we noted that almost the entire volume of CT-β solution was still present, suggestive of an unforeseen complication (*e.g.* blockage) limiting tracer uptake.

3.2. C4 dorsal rhizotomy.

To confirm that the CT-β labeling observed in the mid-cervical dorsal horn reflected phrenic afferent fibers, the “nerve soak” method was preceded by a C4 dorsal rhizotomy in 3 rats. In each of these experiments, robust phrenic motoneuron labeling was present at C4 (Fig. 5A). However, no CT-β positive projections were seen in the C4 dorsal horn or intermediate gray matter (Fig. 5B-C). Phrenic afferent labeling could be detected, however, in the C3 dorsal horn (Fig. 5D-F), and CT-β positive soma were observed in the C3 DRG (Fig. 5G).

3.3. Cascade Blue nerve soak and dual immunochemistry

These additional experiments confirmed that the nerve soak method was successful across two different laboratories. Thus, Cascade Blue nerve soak resulted in robust labeling of cell bodies and neurites of phrenic motoneurons. Mid-cervical histological sections labeled with Cascade Blue and ChAT (a cholinergic marker which effectively identifies motoneurons) are provided in Fig. 6 (top panels). With this approach, it was possible to clearly distinguish between soma and projection fibers that were Cascade Blue positive only (blue), ChAT positive only (red), or dual labeled (white). Cascade Blue positive projections were seen extensively in the cuneate fasciculus of the dorsal white matter in C3-C5 spinal cord in all sections examined. Cascade Blue positive afferents were also prominent in the mid-cervical dorsal horn extending to lamina VI and X; however these projections were never positive for ChAT. Although relatively few in number, Cascade Blue positive afferent projections could be observed in the immediate vicinity of phrenic motor neuron soma. This is most clearly illustrated in the camera lucida drawings that are provided in the bottom panels of Fig. 6. These images are composite drawings based on evaluation of serial sections through each spinal segment; the distribution of phrenic motoneurons and dendritic projections which were positive for both ChAT and Cascade Blue is illustrated in red. Cascade Blue positive projections which were Chat negative are drawn in blue and can be observed in the vicinity of the phrenic motoneuron pool.

To confirm that projections to the deeper spinal lamina do not reflect small diameter presumptive nociceptive C-fibers, tissues were also processed with antibodies against either CGRP or IB4 to label Aδ (type III) or C-fibers (type IV), respectively (Snider and McMahon, 1998). Consistent with prior descriptions of small diameter afferents in the mid-cervical spinal cord (Basbaum *et al.*, 2009; Gibson *et al.*, 1984) staining for CGRP (Fig. 7A) and IB4 (Fig. 7B) was restricted to lamina I-II. However, no dual labeling with Cascade Blue and either CGRP or IB4 was observed at any cervical level.

The C4 DRG was also histologically examined in the Cascade Blue experiments. In addition to Cascade Blue, CGRP and IB4, DRG sections were stained with NeuN to recognize neuronal cell bodies. A representative quadruple-labeled DRG tissue section is shown in Fig. 8A. Cascade Blue-positive neuronal soma can be clearly observed (Fig. 8B), and similar to the CT-β data (Figs. 2-3), this confirms that Cascade Blue is taken up by primary afferent neurons following phrenic nerve soak. In addition, CGRP and IB4 positive cell bodies were present throughout the C4 DRG. Dual labeling with Cascade Blue was noted for IB4 but not CGRP. This suggests that Cascade Blue is capable of labeling A-δ (type III) afferent neurons but as mentioned previously no Cascade Blue-positive afferent projections in the cervical gray matter were co-labeled with IB4 (Fig. 7B).

3.4. Intrapleural / diaphragm delivery of CT-β

Delivery of CT-β between the 5th intercostal space at the anterior axillary line (*i.e.*, “intrapleural labeling”, (Mantilla *et al.*, 2012)) produced extensive and bilateral labeling of phrenic motoneurons (Fig. 9A). The bilateral pattern of labeling suggests that the CT-β solution was dispersed across the entire surface of the diaphragm, probably due to higher concentration of CT-β (1%) as compared to prior studies with this method. In addition, a

limited number CT-β positive fibers could be detected the mid-cervical dorsal horn (Fig. 9B-C), and only a few CT-β positive soma were observed in the C3-C5 DRG soma (Fig. 9G). Thus, the intrapleural delivery method resulted in labeling of afferent projections, but the qualitative density of labeling was reduced when compared to results obtained following direct application of CT-β to the phrenic nerve (*e.g.*, Figs. 2-3 *vs.* Fig. 9). Application of 1% CT-β directly to one side of the diaphragm (*e.g.*, "painting" onto the inferior surface of the diaphragm) produced robust phrenic motoneuron labeling (Fig. 10). However, we were unable to detect any CT-β positive fibers in the dorsal horn of the mid-cervical spinal cord in any rats, and only a few positive cells could be detected in the cervical DRG soma. Following direct diaphragm application, the robust labeling of phrenic motoneurons in the absence of dorsal horn afferent fiber labeling provides further evidence that the dorsal horn labeling observed after "nerve soak" (*e.g.*, Figs. 2-3) does not reflect an artifact due to labeling of phrenic motoneuron dendrites.

3.5. Addition of a transynaptic retrograde tracer

As a final proof-of-concept experiment, we examined if the phrenic nerve soak technique (using CT-β) could be simultaneously combined with a second neuroanatomical tracing approach. Previously, Lane *et al.* used the transynaptic viral tracer PRV to identify cervical interneurons associated with the phrenic motor pool (Lane *et al.*, 2008). Their experiments revealed a population of interneurons that are synaptically coupled to phrenic motoneurons. Prior neurophysiological work current work suggests that phrenic afferents are unlikely to project monosynaptically to phrenic motoneurons (Marlot *et al.*, 1988; Speck, 1987; Speck and Revelette, 1987), and the current work indicates that phrenic afferent projections that terminate in lamina VII-VIII are rare (*e.g.*, Fig. 6). Another possibility is the phrenic afferent projections make polysynaptic projections onto phrenic (or other) spinal motoneuron pools via spinal interneurons. Thus, our intent with these final experiments was to determine if the method developed herein would be useful for future explorations of the spinal neuronal targets of phrenic afferent projections. Fig. 11A shows an example mid-cervical tissue section following simultaneous phrenic nerve soak with both CT-β and PRV. This procedure resulted in PRV-positive interneurons throughout the mid-cervical dorsal horn (Fig. 11B) and the intermediate gray matter (Fig. 11C). Based on the terminal time point of this experiment, the PRV labeled interneurons likely reflected both 2nd and 3rd order retrograde labeling (Lane *et al.*, 2008). CT-β positive phrenic afferent projections can also be observed in lamina III-IV confirming that both interneurons and afferent projections can be histologically identified with this dual labeling approach.

4. Discussion

We found that a "nerve soak" approach for delivering transganglionic tracers to the phrenic nerve was effective at labeling phrenic afferent projections in the cervical spinal cord. The method was successful across two independent laboratories, and two different tracers. The results also serve to verify and extend a few earlier histological studies. Specifically, the pattern of phrenic afferent labeling was consistent with an earlier report (Goshgarian and Roubal, 1986a), but more extensive afferent projections were observed including fibers in lamina V-VII and X. Another unique feature of these data was the observation of phrenic

afferent projections in lamina IX in the immediate vicinity of the phrenic motoneuron pool in the adult rat. We also demonstrated that the method can be successfully combined with a transynaptic tracer, and therefore provides a method for histologically examining the relationship of phrenic afferent projections and interneurons which are synaptically coupled to the phrenic motoneuron pool. This is motivated by prior neurophysiological data suggesting that activation of phrenic afferent neurons can impact propriospinal neuronal activity (Cleland and Getting, 1993; Iscoe and Duffin, 1996; Road *et al.*, 1993; Speck and Revelette, 1987).

4.1. Comparison to published histological studies of phrenic afferents.

Larnical *et al.* applied a tracer (fast blue) directly to the phrenic nerve in cats and coupled this with cervical dorsal column injection of another tracer (nuclear yellow) (Larnicol *et al.*, 1984). A small number of neuronal soma in dorsal root ganglia were co-labeled, and the authors concluded that these were most likely type Ia and Ib afferents from diaphragm receptors. Goshgarian and Roubal (1986) were able to identify myelinated phrenic afferent fibers by applying horseradish peroxidase (HRP) crystals to the phrenic nerve in adult rats. In their study, DRG labeling was observed at the C3-C7 segmental levels, and afferent projections were seen in C4-C5 lamina I-IV. In contrast, the CT-β or Cascade Blue nerve soak method resulted in labeling of afferents with dense arborization and deeper laminar projections (*e.g.*, Figs. 2-5). In addition, we observed phrenic afferent fibers in the C3 spinal cord, whereas HRP labeling was absent at that segmental level in the prior study (Goshgarian and Roubal, 1986a). The suggestion of improved afferent labeling using the current approach as compared to the HRP method is supported by data from Lindsey *et al.* who were unable to label phrenic afferents in rats using HRP (Lindsay *et al.*, 1991).

Song and colleagues showed that phrenic afferents robustly projected to lamina IX of the cervical spinal cord in neonatal rats (Song *et al.*, 1999), a finding consistent with monosynaptic connections between phrenic afferents and phrenic motoneurons. The Cascade Blue method revealed a few phrenic afferent projections to lamina IX, but not nearly to the extent reported in the Song *et al.* experiments. There are a several possible explanations for the differences between that study, the current data and prior work (Goshgarian and Roubal, 1986a). First and most importantly, Song *et al.* studied rats at very early developmental stages (*e.g.*, prenatal and a few days post-natal). Thus, phrenic afferent projections to the spinal cord may be more extensive, and extend to deeper lamina, at earlier developmental stages. Dramatic changes in phrenic motoneuron morphology and biophysical properties occur during developmental stages (Greer *et al.*, 1999), and alterations in the afferent innervation of these cells may change during development. In that regard, it should be noted that connections from phrenic afferents to phrenic motoneurons have not been detected neurophysiologically in adult mammals (Macron *et al.*, 1988; Marlot *et al.*, 1988; Speck, 1987; Speck and Revelette, 1987). Second, the carbo-cyanine dye (Dil) method used by Song *et al.* required a considerable period of incubation (*e.g.*, 4-20 weeks) before tissues were harvested and histologically evaluated. The prolonged incubation may have enabled more robust detection of afferent projections *vs.* the current method. Alternatively the Dil may have diffused across cell membrane and labelled interneurons, and this possibility was also noted by the original authors (Song *et al.*, 1999).

4.2. Use of CT-β and Cascade Blue to trace afferent neuronal projections

An electron microscopy study of the rat phrenic nerve reported that 57% of fibers were myelinated and 43% were unmyelinated (Langford and Schmidt, 1983). Thus, in the context of the current results, an important question is whether the labeled afferents were myelinated or unmyelinated. The IB4 or CGRP immunochemistry results indicate that the Cascade Blue labeled neurons were unmyelinated. None of the small diameter afferents in lamina I-II which were IB4 or CGRP positive were also positive for Cascade Blue. In regards to the CT-β results, prior studies establish that CT-β binds to a ganglioside molecule (GM1) in myelinated fibers and this enables uptake and subsequent transport along the axon (Cuatrecasas, 1973; Holmgren *et al.*, 1973; King and Van Heyningen, 1973). For example, Robertson and Perry (1991) showed that CT-β binds and is transported almost exclusively in DRG neurons that have myelinated processes with relatively fast conduction velocities (Robertson *et al.*, 1991). There is, however, one published exception in which CT-β labeling was noted in non-myelinated C-fibers projecting from the bladder in L6-S1 spinal cord (Wang *et al.*, 1998). In addition, long-term peripheral nerve injury (*e.g.*, > 2-wks) can also produce a state in which damaged C-fiber afferents acquire the capacity for CT-β uptake (Shehab *et al.*, 2003; Tong *et al.*, 1999). Tong et al (1999) showed that 20 days following peripheral nerve injury, CT-β DRG neuronal labeling in both monkeys and rats was apparent in non-myelinated fibers, and this was not seen in the absence of peripheral nerve injury.

Based on the topographical distribution of the phrenic afferents observed in our study, the ChAT labeling in the Cascade Blue experiments, and prior studies with CT-β (Cuatrecasas, 1973; Holmgren *et al.*, 1973; King and Van Heyningen, 1973), we suggest that the majority of afferent fibers described herein are myelinated fibers. Many independent laboratories have confirmed that the phrenic nerve contains myelinated fibers (Banzett *et al.*, 1981; Corda *et al.*, 1965a; Fryman and Frazier, 1987; Glebovskii, 1962; Holt *et al.*, 1991; Marlot *et al.*, 1985), and in our study the afferent distribution patterns observed in lamina IV-VII and X are most consistent with myelinated afferents. However, a few DRG neurons were dual labeled for Cascade Blue and IB-4, a result suggesting that Cascade Blue is capable of labeling A-δ (type III) afferent neurons. However, no Cascade Blue-positive afferent projections in the cervical gray matter could be detected that were co-labeled with IB4.

4.3. Interpretational issues

The primary intent of using two different transganglionic tracers across two different laboratories was to confirm that the approach of “nerve soak” was robust and reproducible. However, this also afforded the opportunity for a qualitative comparison of the afferent labeling achieved with CT-β *vs.* Cascade Blue. One apparent difference between the two tracers was in the relative extent of dorsal column white matter labeling. The Cascade Blue experiments produced a qualitatively greater density of labeled afferent fibers in the area of the cuneate fasciculus (*e.g.*, Fig. 3 *vs.* Fig. 6). We also observed that Cascade Blue, but not CT-β, labeling of phrenic afferent projections in the immediate vicinity of the phrenic motor nucleus (*e.g.*, lamina IX, Fig. 6). The specific reasons for the potentially enhanced phrenic afferent labeling with Cascade Blue are not clear, but may relate to the lower molecular weight of this molecule (~ 3 kDa) as compared to CT-β (~11.5 kDa).

Another consideration is that the phrenic nerve contains unmyelinated sympathetic and non-diaphragmatic mediastinal afferent fibers (Balkowiec and Szulczyk, 1992; Capps, 1932; Green, 1902; Iwahashi *et al.*, 1991; Kostreva and Pontus, 1993; Ruckebusch, 1961). Most of these projections join the phrenic nerve near the heart (Razook *et al.*, 1995). With the nerve soak method, transganglionic tracers were applied to the phrenic nerve at the level of brachial plexus (*i.e.*, "upstream" from the heart). Therefore, if unmyelinated fibers were labeled with our method, they may represent both diaphragmatic and non-diaphragmatic fibers. However, as noted earlier, the data are most consistent with labeling of myelinated primary afferent fibers. Finally, it should be mentioned that anatomical differences exist between the left and right phrenic nerves (Hebb *et al.*, 1964; Laskowski *et al.*, 1991; Song *et al.*, 1999). For example, Song *et al.* reported approximately 20% more axons in the right *vs.* left phrenic nerve (Song *et al.*, 1999). Here we only studied the left phrenic nerve since our primary intent was to validate the technique.

4.4. Summary and Conclusions

Application of CT-β or Cascade Blue to the phrenic nerve results in robust immunoreactivity in C3-C5 DRG cell bodies and afferent fibers in the dorsal mid-cervical spinal cord. Direct application of CT-β to the phrenic nerve produced much more consistent labeling of afferent projections as compared to intrapleural delivery, and in our experiments direct diaphragm application of CT-β did not label any afferent projections. Thus, the "nerve soak" method described herein effectively labels phrenic afferent neurons, and will be useful for mapping the spinal projections of phrenic afferent neurons in health and disease (*e.g.*, after spinal cord injury (Vinit *et al.*, 2007)).

Acknowledgements.

We are grateful for the excellent histological and immunochemistry assistance of Marda Jorgenson. Funding was provided by NIH 1R01NS080180-01A1 (DDF), NIH 1 R01 NS054025-06 (PJR), 1R01 NS081112 (MAL), PO1 NS 055976 (MAL), and the State of Florida Brain and Spinal Cord Injury Research Trust Fund (DDF and PJR) awarded through the McKnight Brain Institute at the University of Florida. PRV614 was produced and supplied by Dr David Bloom (University of Florida). Primary antibodies to PRV were supplied by Lynn Enquist (Princeton University) as part of Virus Center funding (P40RR018604) awarded to Dr Enquist.

Reference

Balkowiec A, Szulczyk P, 1992 Properties of postganglionic sympathetic neurons with axons in phrenic nerve. Respir Physiol 88, 323–331. [PubMed: 1615229]

Banzett RB, Inbar GF, Brown R, Goldman M, Rossier A, Mead J, 1981 Diaphragm electrical activity during negative lower torso pressure in quadriplegic men. J Appl Physiol Respir Environ Exerc Physiol 51, 654–659. [PubMed: 7327967]

Basbaum AI, Bautista DM, Scherrer G, Julius D, 2009 Cellular and molecular mechanisms of pain. Cell 139, 267–284. [PubMed: 19837031]

Bolser DC, Hobbs SF, Chandler MJ, Foreman RD, 1991 Inhibitory effects of phrenic afferent fibers on primate lumbosacral spinothalamic tract neurons. Brain Res 557, 162–166. [PubMed: 1747751]

Capps, 1932 An Experimental and Clinical Study of Pain in the Pleura. Pericardium and Peritoneum. Macmillan, New York.

Cleland CL, Getting PA, 1993 Respiratory-modulated and phrenic afferent-driven neurons in the cervical spinal cord (C4-C6) of the fluorocarbon-perfused guinea pig. Exp Brain Res 93, 307–311. [PubMed: 8491269]

Corda M, Eklund G, Euler C.v., 1965a External Intercostal and Phrenic a Motor Responses to Changes in Respiratory Load. Acta Physiologica Scandinavica 63, 391–400. [PubMed: 14324074]

Corda M, Voneuler C, Lennerstrand G, 1965b Proprioceptive Innervation of the Diaphragm. J Physiol 178, 161–177. [PubMed: 14298107]

Cuatrecasas P, 1973 Gangliosides and membrane receptors for cholera toxin. Biochemistry 12, 3558–3566. [PubMed: 4731192]

Davenport PW, Thompson FJ, Reep RL, Freed AN, 1985 Projection of phrenic nerve afferents to the cat sensorimotor cortex. Brain Res 328, 150–153. [PubMed: 3971173]

De Troyer AD, 1998 The canine phrenic-to-intercostal reflex. J Physiol 508, 919–927. [PubMed: 9518742]

Dobbins EG, Feldman JL, 1994 Brainstem network controlling descending drive to phrenic motoneurons in rat. J Comp Neurol 347, 64–86. [PubMed: 7798382]

Duron B, Jung-Caillol MC, Marlot D, 1978 Myelinated nerve fiber supply and muscle spindles in the respiratory muscles of cat: quantitative study. Anatomy and embryology 152, 171–192. [PubMed: 147637]

Duron B, Marlot D, 1980 The non-myelinated fibers of the phrenic and the intercostal nerves in the cat. Z Mikrosk Anat Forsch 94, 257–268. [PubMed: 7415394]

Formenti A, Zocchi L, 2014 Error signals as powerful stimuli for the operant conditioning-like process of the fictive respiratory output in a brainstem-spinal cord preparation from rats. Behavioural Brain Research 272, 8–15. [PubMed: 24978097]

Fryman DL, Frazier DT, 1987 Diaphragm afferent modulation of phrenic motor drive. J Appl Physiol 62, 2436–2441. [PubMed: 3610938]

Gibson SJ, Polak JM, Bloom SR, Sabate IM, Mulderry PM, Ghatei MA, McGregor GP, Morrison JF, Kelly JS, Evans RM, et al., 1984 Calcitonin gene-related peptide immunoreactivity in the spinal cord of man and of eight other species. The Journal of neuroscience : the official journal of the Society for Neuroscience 4, 3101–3111. [PubMed: 6209366]

Glebovskii VD, 1962 [On stretch receptors of the diaphragm]. Fiziologicheskii zhurnal SSSR imeni I. M. Sechenova 48, 545–553.

Goshgarian HG, Ellenberger HH, Feldman JL, 1991 Decussation of bulbospinal respiratory axons at the level of the phrenic nuclei in adult rats: a possible substrate for the crossed phrenic phenomenon. Exp Neurol 111, 135–139. [PubMed: 1984430]

Goshgarian HG, Roubal PJ, 1986a Origin and distribution of phrenic primary afferent nerve fibers in the spinal cord of the adult rat. Experimental Neurology 92, 624–638. [PubMed: 3709737]

Goshgarian HG, Roubal PJ, 1986b Origin and distribution of phrenic primary afferent nerve fibers in the spinal cord of the adult rat. Experimental neurology 92, 624–638. [PubMed: 3709737]

Gottschall J, 1981 The diaphragm of the rat and its innervation. Muscle fiber composition; perikarya and axons of efferent and afferent neurons. Anat Embryol (Berl) 161, 405–417. [PubMed: 7247037]

Green S, 1902 Phrenic nerve injuries. Anatomical and experimental research. Am. J. Med. Sci 123, 196–220.

Greer JJ, Allan DW, Martin-Caraballo M, Lemke RP, 1999 An overview of phrenic nerve and diaphragm muscle development in the perinatal rat. Journal of Applied Physiology 86, 779–786. [PubMed: 10066685]

Hebb CO, Krnjevic K, Silver A, 1964 ACETYLCHOLINE AND CHOLINE ACETYLTRANSFERASE IN THE DIAPHRAGM OF THE RAT. J Physiol 171, 504–513. [PubMed: 14193937]

Holmgren J, Lonnroth I, Svennerholm L, 1973 Tissue receptor for cholera exotoxin: postulated structure from studies with GM1 ganglioside and related glycolipids. Infect Immun 8, 208–214. [PubMed: 4125267]

Holt GA, Dalziel DJ, Davenport PW, 1991 The transduction properties of diaphragmatic mechanoreceptors. Neurosci Lett 122, 117–121. [PubMed: 2057127]

Hussain SN, Chatillon A, Comtois A, Roussos C, Magder S, 1991 Chemical activation of thin-fiber phrenic afferents. 2. Cardiovascular responses. Journal of Applied Physiology 70, 77–86. [PubMed: 2010412]

Iscoe S, Duffin J, 1996 Effects of stimulation of phrenic afferents on cervical respiratory interneurones and phrenic motoneurones in cats. The Journal of Physiology 497, 803–812. [PubMed: 9003565]

Iwahashi K, Matsuda R, Tsunekawa K, 1991 Afferent innervation of the gallbladder in the cat, studied by the horseradish peroxidase method. J Auton Nerv Syst 32, 145–151. [PubMed: 2030260]

Jammes Y, Buchler B, Delpierre S, Rasidakis A, Grimaud C, Roussos C, 1986 Phrenic afferents and their role in inspiratory control. J Appl Physiol 60, 854–860. [PubMed: 3957836]

King CA, Van Heyningen WE, 1973 Deactivation of cholera toxin by a sialidase-resistant monosialosylganglioside. J Infect Dis 127, 639–647. [PubMed: 4707310]

Kostreva DR, Pontus SP, 1993 Hepatic vein, hepatic parenchymal, and inferior vena caval mechanoreceptors with phrenic afferents. Am J Physiol 265, G15–20. [PubMed: 8338164]

Landau BR, Akert K, Roberts TS, 1962 Studies on the innervation of the diaphragm. The Journal of Comparative Neurology 119, 1–10.

Lane MA, White TE, Coutts MA, Jones AL, Sandhu MS, Bloom DC, Bolser DC, Yates BJ, Fuller DD, Reier PJ, 2008 Cervical prephrenic interneurons in the normal and lesioned spinal cord of the adult rat. The Journal of comparative neurology 511, 692–709. [PubMed: 18924146]

Langford LA, Schmidt RF, 1983 An electron microscopic analysis of the left phrenic nerve in the rat. Anat Rec 205, 207–213. [PubMed: 6846871]

Larnicol N, Rose D, Duron B, 1984 Identification of phrenic afferents in the dorsal columns: a fluorescent double-labeling study in the cat. Neurosci Lett 52, 49–53. [PubMed: 6527837]

Laskowski MB, Norton AS, Berger PK, 1991 Branching patterns of the rat phrenic nerve during development and reinnervation. Exp Neurol 113, 212–220. [PubMed: 1868904]

Lindsay AD, Greer JJ, Feldman JL, 1991 Phrenic motoneuron morphology in the neonatal rat. The Journal of Comparative Neurology 308, 169–179. [PubMed: 1716267]

Macron JM, Marlot D, Wallois F, Duron B, 1988 Phrenic-to-phrenic inhibition and excitation in spinal cats. Neuroscience Letters 91, 24–29. [PubMed: 3173784]

Mantilla CB, Bailey JP, Zhan WZ, Sieck GC, 2012 Phrenic motoneuron expression of serotonergic and glutamatergic receptors following upper cervical spinal cord injury. Experimental neurology 234, 191–199. [PubMed: 22227062]

Mantilla CB, Zhan WZ, Sieck GC, 2009 Retrograde labeling of phrenic motoneurons by intrapleural injection. J Neurosci Methods 182, 244–249. [PubMed: 19559048]

Marlot D, Macron J-M, Duron B, 1985 Projection of phrenic afferents to the external cuneate nucleus in the cat. Brain Research 327, 328–330. [PubMed: 2985178]

Marlot D, Macron J-M, Duron B, 1988 Effects of ipsilateral and contralateral cervical phrenic afferents stimulation on phrenic motor unit activity in the cat. Brain Research 450, 373–377. [PubMed: 3401718]

National Research Council Committee on Guidelines for the Use of Animals in Neuroscience and Behavioral, R., (2003). The National Academies Collection: Reports funded by National Institutes of Health, Guidelines for the Care and Use of Mammals in Neuroscience and Behavioral Research. National Academies Press (US) National Academy of Sciences, Washington (DC).

Razook JC, Chandler MJ, Foreman RD, 1995 Phrenic afferent input excites C1-C2 spinal neurons in rats. Pain 63, 117–125. [PubMed: 8577482]

Road JD, Osborne S, Wakai Y, 1993 Delayed poststimulus decrease of phrenic motoneuron output produced by phrenic nerve afferent stimulation. J Appl Physiol 74, 68–72. [PubMed: 8444737]

Robertson B, Perry MJ, Lawson SN, 1991 Populations of rat spinal primary afferent neurons with choleragenoid binding compared with those labelled by markers for neurofilament and carbohydrate groups: a quantitative immunocytochemical study. Journal of Neurocytology 20, 387–395. [PubMed: 1869879]

Ruckebusch Y, 1961 Influx afferents d'origine perocardique dans les nerfs phreniques. C.R. Soc Biol 155, 161–178.

Shehab SA, Spike RC, Todd AJ, 2003 Evidence against cholera toxin B subunit as a reliable tracer for sprouting of primary afferents following peripheral nerve injury. Brain Res 964, 218–227. [PubMed: 12576182]

Shehab SA, Spike RC, Todd AJ, 2004 Do central terminals of intact myelinated primary afferents sprout into the superficial dorsal horn of rat spinal cord after injury to a neighboring peripheral nerve? J Comp Neurol 474, 427–437. [PubMed: 15174085]

Snider WD, McMahon SB, 1998 Tackling pain at the source: new ideas about nociceptors. Neuron 20, 629–632. [PubMed: 9581756]

Song A, Tracey DJ, Ashwell KW, 1999 Development of the rat phrenic nerve and the terminal distribution of phrenic afferents in the cervical cord. Anat Embryol (Berl) 200, 625–643. [PubMed: 10592066]

Speck DF, 1987 Supraspinal involvement in the phrenic-to-phrenic inhibitory reflex. Brain Research 414, 169–172. [PubMed: 3620920]

Speck DF, Revelette WR, 1987 Attenuation of phrenic motor discharge by phrenic nerve afferents. Journal of Applied Physiology 62, 941–945. [PubMed: 3571092]

Tong YG, Wang HF, Ju G, Grant G, Hokfelt T, Zhang X, 1999 Increased uptake and transport of cholera toxin B-subunit in dorsal root ganglion neurons after peripheral axotomy: possible implications for sensory sprouting. J Comp Neurol 404, 143–158. [PubMed: 9934990]

Vinit S, Stamegna JC, Boulenguez P, Gauthier P, Kastner A, 2007 Restorative respiratory pathways after partial cervical spinal cord injury: role of ipsilateral phrenic afferents. Eur J Neurosci 25, 3551–3560. [PubMed: 17610574]

Wall PD, Kerr BJ, Ramer MS, 2002 Primary afferent input to and receptive field properties of cells in rat lumbar area X. J Comp Neurol 449, 298–306. [PubMed: 12115681]

Wang HF, Shortland P, Park MJ, Grant G, 1998 Retrograde and transganglionic transport of horseradish peroxidase-conjugated cholera toxin B subunit, wheatgerm agglutinin and isolectin B4 from Griffonia simplicifolia I in primary afferent neurons innervating the rat urinary bladder. Neuroscience 87, 275–288. [PubMed: 9722157]

Zhang W, Davenport PW, 2003 Activation of thalamic ventroposteriolateral neurons by phrenic nerve afferents in cats and rats. Journal of Applied Physiology 94, 220–226. [PubMed: 12391131]

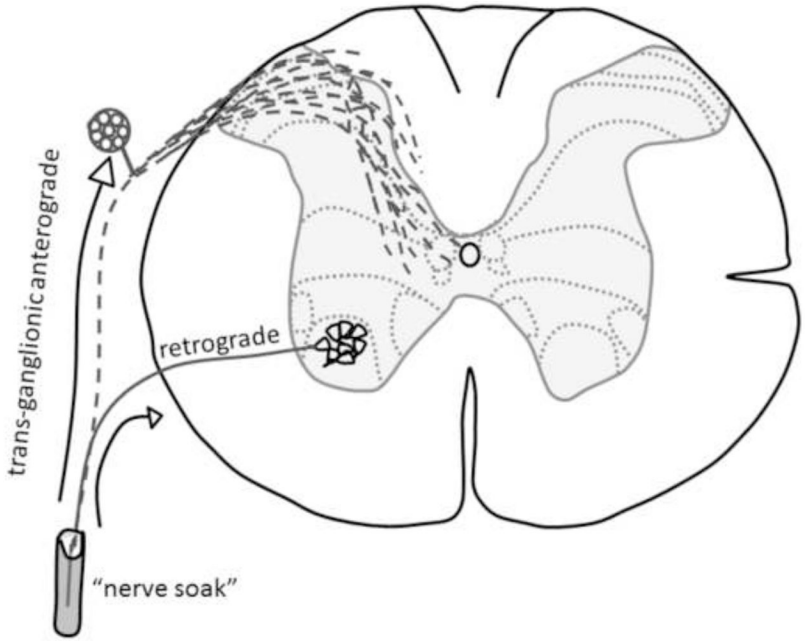

Figure 1. Schematic showing pathway of CT-β or Cascade Blue movement following application to the phrenic nerve.

Tissues were harvested for histological evaluation at 96-hrs following initiation of the nerve soak procedure.

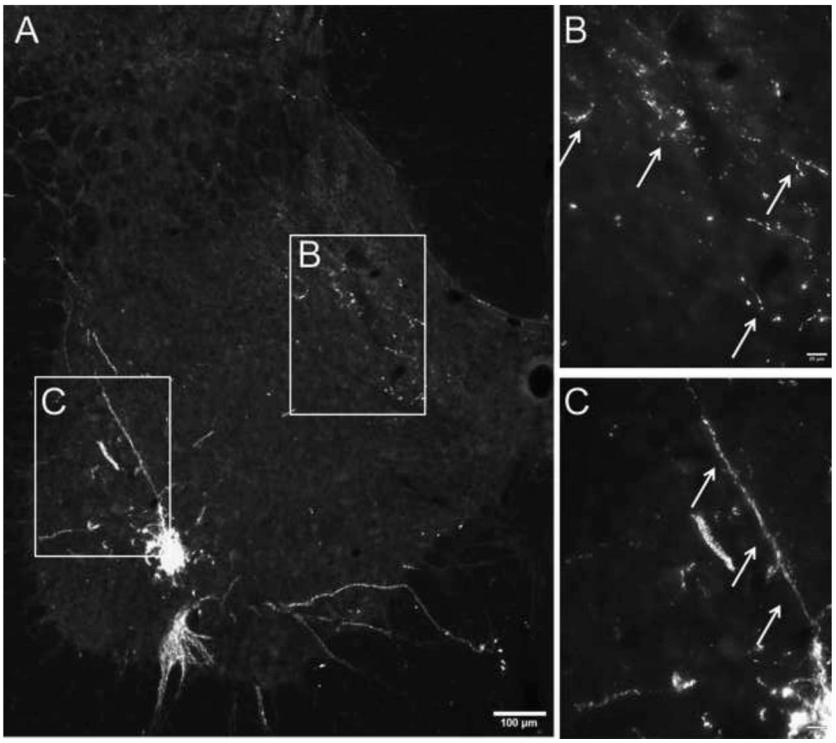

Figure 2. Phrenic afferent fiber *vs.* phrenic motoneuron dendrite labeling following CT-β application to the phrenic nerve.

Panel A shows a view of the left half of the C4 spinal cord; the areas highlighted by the boxes are shown at higher magnification in panels B and C. CT-β labelled afferent projections in the dorsal spinal cord were distinct in appearance from the CT-β labelled phrenic motoneuron dendritic projections. Phrenic afferent fibers were thinner with a relatively diffuse distribution of "punctate" synaptic terminals (B). In contrast, the phrenic motoneuron dendrites were more linear in appearance, and could be observed radiating from the cell soma (C). Another demarcating feature was the size of the dendritic boutons which were smaller compared to more bulbous synaptic boutons associated with the terminal endings of afferent fibers. Scale bars: 100μm (A) or 20μm (B-C).

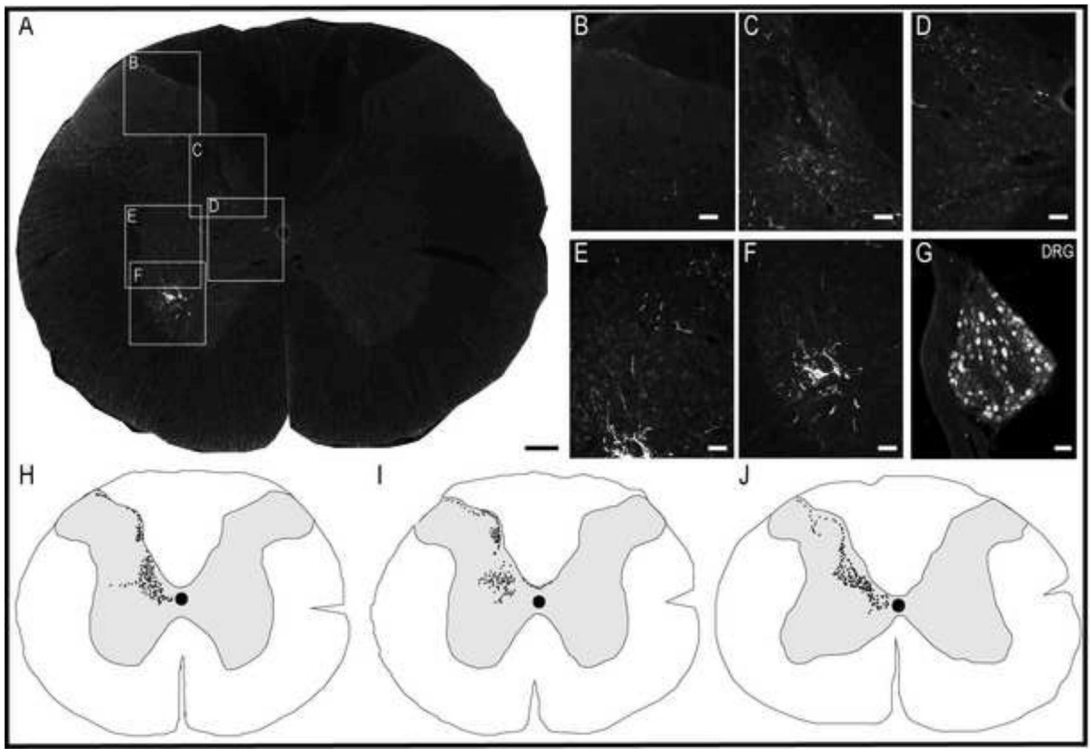

Figure 3. Histological examples of phrenic motoneuron and afferent fiber labeling following CT-β application to the phrenic nerve.

Panel A provides a representative image of the C3 spinal cord; the areas highlighted by the boxes are shown at higher magnification in panels B-F. Robust labeling of phrenic motoneurons can be readily observed in A, along with punctate labeling of afferent projections in the dorsal gray matter. Panel B shows CT-β positive afferent projections in laminae II-III; higher magnification views of afferent fibers in laminae IV-VI-VII and IX are provided in C and D, respectively. Afferent projections extending into lamina VII can be appreciated in E-F. Panel G shows a 30μm section of the C3 dorsal root ganglion ipsilateral to the injection; the positive labeling of cell bodies confirms labeling of sensory afferent neurons. Panels H-J are camera lucida style images from the C3-C5 spinal cord which illustrate the pattern of CT-β labeling of cervical afferent fibers obtained using this technique. Note the consistent presence of afferent projections in laminae I-VII, extending into lamina X. Scale bars: 200μm (A), 50μm (B-F) and 10μm (G).

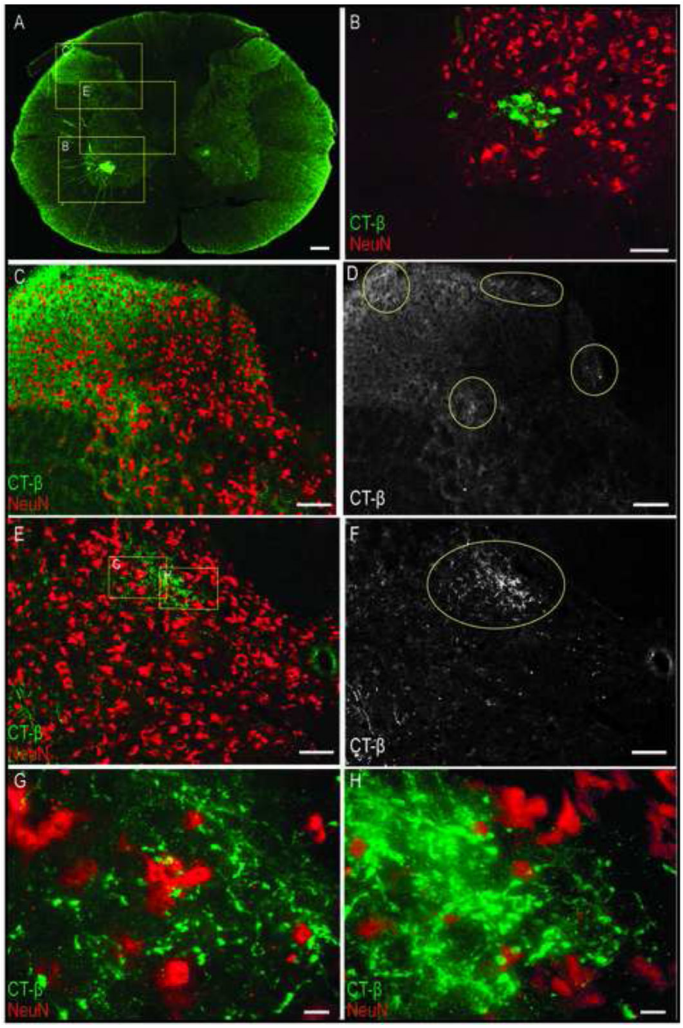

Figure 4. Confocal microscopy image of phrenic motoneuron and afferent fiber labeling in the C4 spinal cord following CT-β phrenic nerve application.

In this example, CT-β labelled phrenic afferents were visualized using a secondary antibody with green fluorescence, and a neuron specific marker (NeuN) was visualized with a red fluorescent secondary antibody. The punctate CT-β labeling of phrenic afferent projections can be observed in the dorsal horn (C) and intermediate grey region (E). Panels D and F were created to better highlight these projections, and show monochrome images derived from the original images using Image-J software. The monochrome images clearly show the afferent fiber projection (highlighted by the circles in D and F). The higher magnification shown in panels G and H illustrates the distinct morphological characteristics of CT-β positive terminal synaptic boutons. Scale bars: 200μm (A), 100μm (B-F), and 10 μm (G-H).

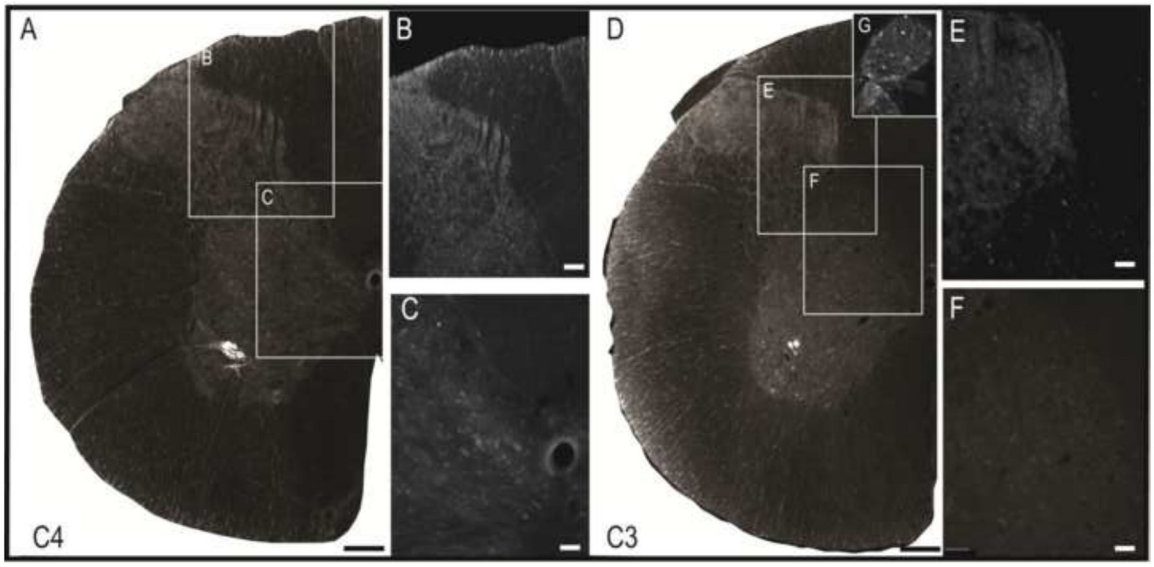

Figure 5. Absence of C4 phrenic afferent labeling when CT-β phrenic nerve application is preceded by C4 dorsal rhizotomy.

Rhizotomy was performed at C4 prior to the CT-β application to confirm that the labeled axons were afferents. Representative images of the C4 and C3 spinal cord are provided. There was total absence of afferent labeling at C4 as shown in Panels A-C. In contrast, CT-β positive afferent fiber labeling can be observed at C3 (Panels D-F), and CT-β positive soma were seen in the C3 dorsal root ganglion (panel G). Scale bars represent 200μm (A, D) or 50μm (B-C, E-F).

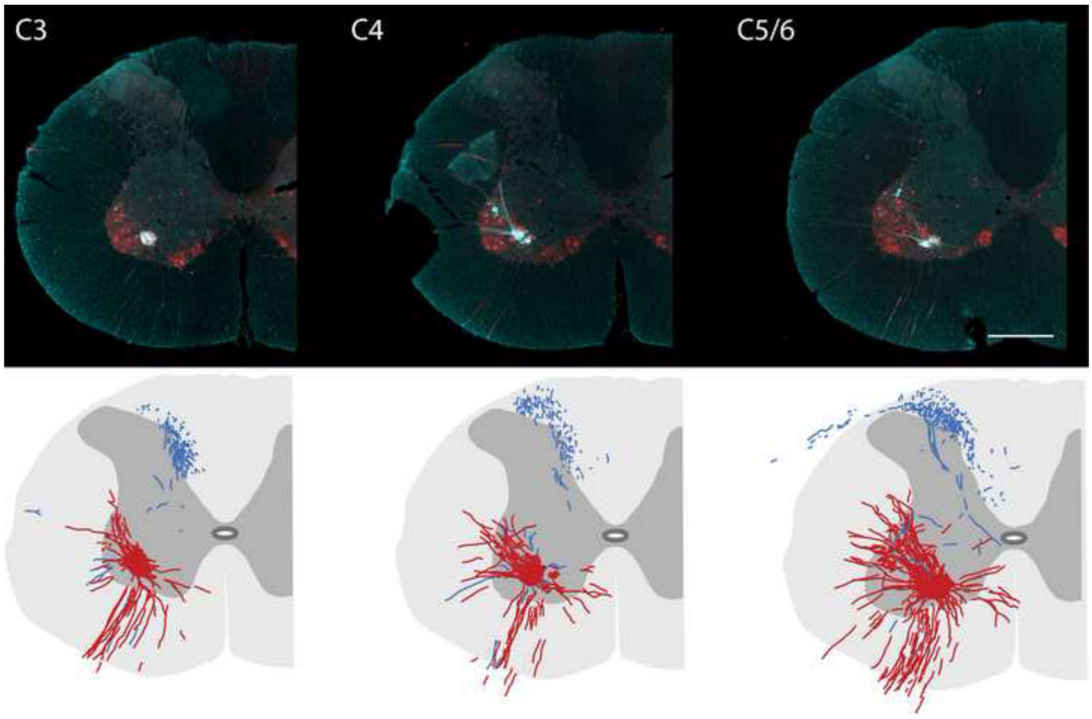

Figure 6. Representative cross sections (40 μm) of the cervical spinal cord ipsilateral to the phrenic nerve following tracing with Cascade Blue.

Representative tissue sections that were dual-labeled with Cascade Blue and ChAT are provided from the C3 (A), C4 (B) and C5/6 (C) spinal cord. The images are pseudocoloured in turquoise for optimal contrast, and reveal the distribution of Cascade Blue labeled afferents relative to motoneuron (and dendritic) labeling. Sections were selected 200 μm apart from each of these cervical regions and used to create the camera lucida images shown in Panels D-F. In these images, phrenic afferents are shown in blue (*i.e.*, cascade blue only labeled fibers) and phrenic motoneurons are shown in red (representing dual Cascade blue / ChAT labeled cells and neurites). Scale bar is 250μm

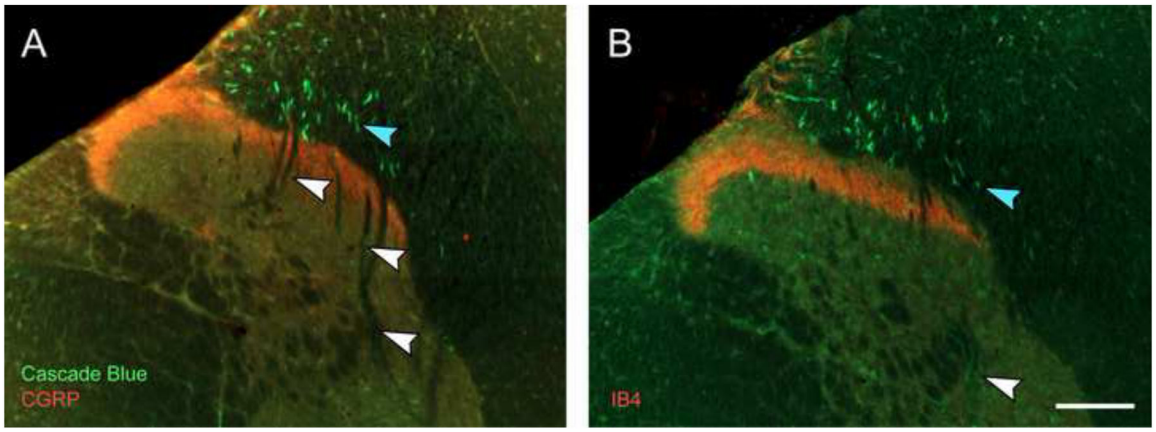

Figure 7. Histological examples of Cascade Blue afferent labeling (green) relative to CGRP (A, red) or IB4 (B, red) afferent labeling.

No Cascade Blue afferents were seen to be dual-labeled with either CGRP or IB4. Note the relative distribution of larger (blue arrowheads) and smaller (white arrowheads) Cascade Blue afferents. Scale bar is 100μm.

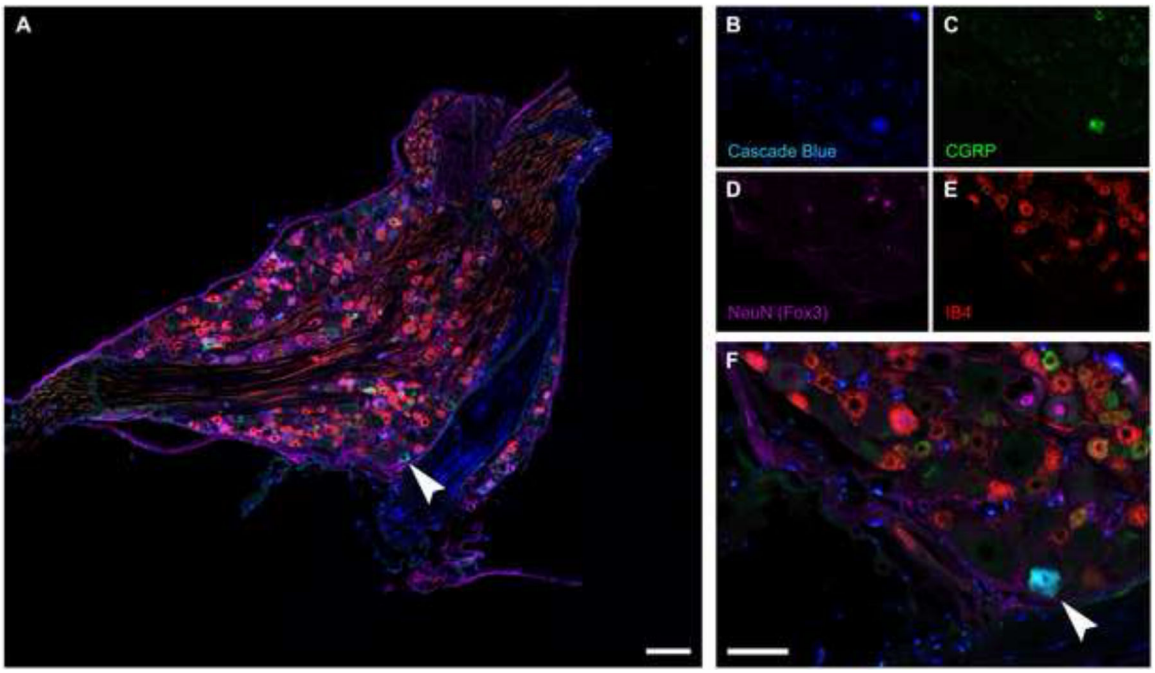

Figure 8. Cascade Blue labeled DRG neurons.

Sections (10 μm) through the dorsal root ganglion were immunolabeled for Cascade Blue (blue), CGRP (green), IB4 (red) and NeuN (Fox3, purple). Note that not all DRG neurons were NeuN positive. While no dual IB4-Cascade Blue neurons were observed, several dual CGRP-Cascade Blue labeled DRG cells were observed (arrowhead). Scale bar indicates 100μm (A), 400μm (B-E), or 200μm (F)

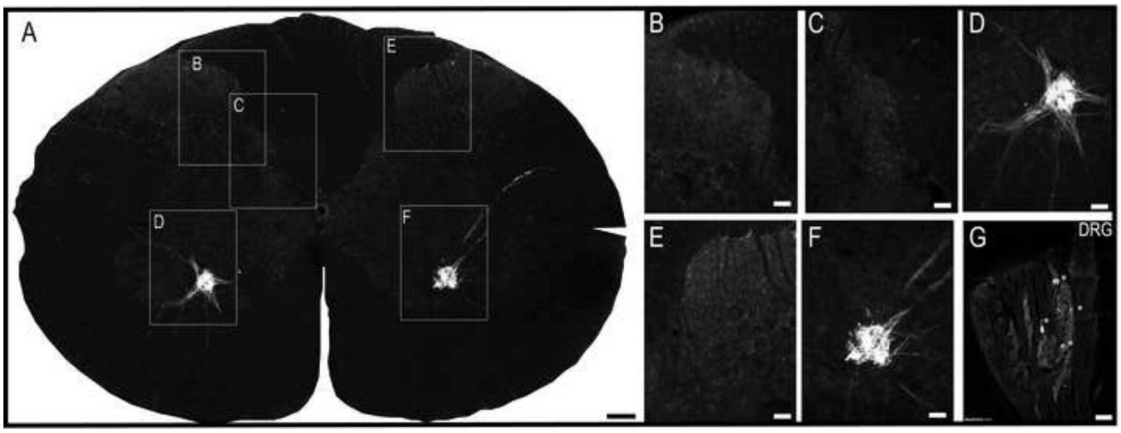

Figure 9. Histological examples of phrenic motoneuron and afferent fiber labeling following delivery of CT-β to the intrapleural space.

Robust labeling of phrenic motoneurons was observed on both sides of the spinal cord (D, F). Sparse labeling of afferent fibers was detected bilaterally (B, C, E), and a few CT-β labeled cells could be observed in the dorsal root ganglion on the left side (indicated by * in panel G). The example shown is from the C5 spinal cord. Scale bars indicate 200μm (A), 50μm (B-F) or 10μm (G).

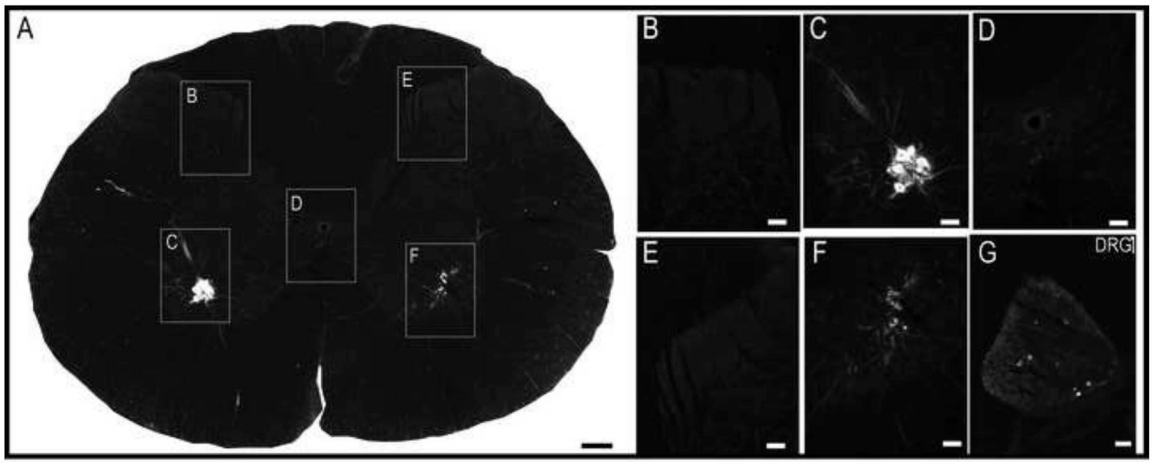

Figure 10. Histological examples of phrenic motoneuron labeling following application of CT-β to the diaphragm.

This technique very robustly labeled phrenic motoneurons (C). However, afferent fiber labeling in the dorsal horn could not be detected (B,E), and we noted some sparse labeling near the central canal (D) and occasional labeling of dorsal root ganglion cells on the left side (indicated by * in panel G). The example shown is from the C4 spinal cord. Scale bars represent 200μm (A), 50μm (B-F) or 10μm (G).

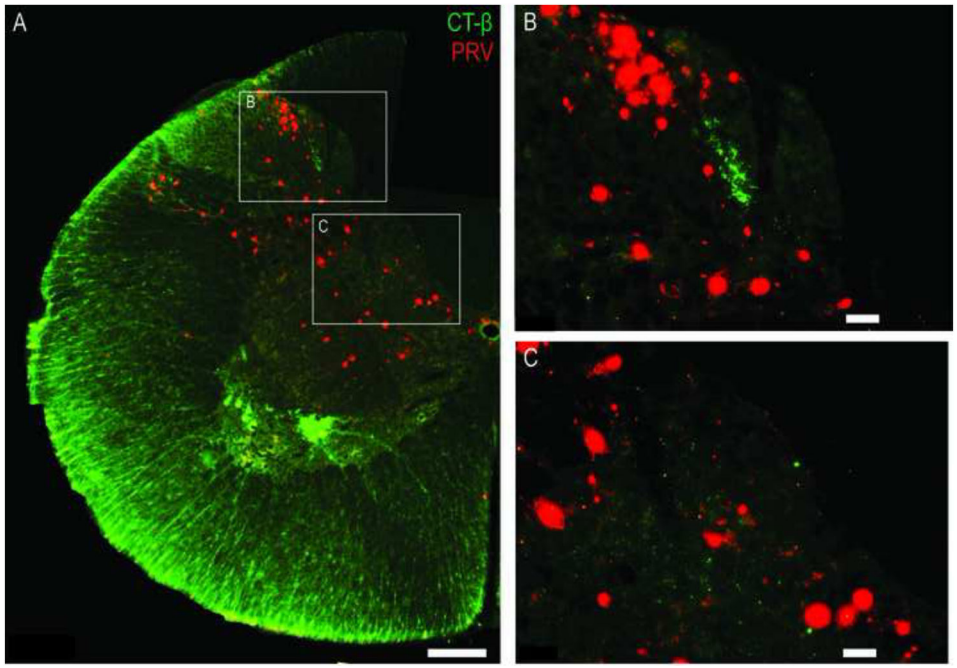

Figure 11. Combined delivery of CT-β and PRV to the phrenic nerve.

The histological examples demonstrate successful combination of the CT-β labeling method with transynaptic labeling of cervical spinal cord neurons using PRV. In this example, CT-β labeled afferent fibers are shown in green, and the trans-synaptically labeled interneurons are red. Scale bars indicate 200μm (A) or 50μm (B-C).